SAR3419: An Anti-CD19-Maytansinoid Immunoconjugate for the Treatment of B-Cell Malignancies

Veronique Blanc[1], Anne Bousseau[1], Anne Caron[1], Chantal Carrez[1], Robert J. Lutz[2], and John M. Lambert[2]

Abstract

SAR3419 is a novel anti-CD19 humanized monoclonal antibody conjugated to a maytansine derivate through a cleavable linker for the treatment of B-cell malignancies. SAR3419 combines the strengths of a high-potency tubulin inhibitor and the exquisite B-cell selectivity of an anti-CD19 antibody. The internalization and processing of SAR3419, following its binding at the surface of CD19-positive human lymphoma cell lines and xenograft models, release active metabolites that trigger cell-cycle arrest and apoptosis, leading to cell death and tumor regression. SAR3419 has also been shown to be active in different lymphoma xenograft models, including aggressive diffuse large B-cell lymphoma, resulting in complete regressions and tumor-free survival. In these models, the activity of SAR3419 compared favorably with rituximab and lymphoma standard of care chemotherapy. Two phase I trials with 2 different schedules of SAR3419 as a single agent were conducted in refractory/relapsed B-cell non-Hodgkin lymphoma. Activity was reported in both schedules, in heavily pretreated patients of both follicular and diffuse large B-cell lymphoma subtypes, with a notable lack of significant hematological toxicity, validating SAR3419 as an effective antibody-drug conjugate and opening opportunities in the future. Numerous B-cell–specific anti-CD19 biologics are available to treat B-cell non-Hodgkin lymphoma, and early phase I results obtained with SAR3419 suggest that it is a promising candidate for further development in this disease. In addition, thanks to the broad expression of CD19, SAR3419 may provide treatment options for B-cell leukemias that are often CD20-negative. *Clin Cancer Res; 17(20); 6448–58. ©2011 AACR.*

Introduction

Non-Hodgkin lymphoma (NHL) is the most common lymphoma, with an estimated 65,540 new cases and 20,210 deaths registered in the United States in 2010 (1). NHL originates from the malignant development of B or T lymphocytes and comprises a heterogeneous group of malignancies (2), among which B-cell lymphomas account for 85% of all cases (3). Despite the significant improvement in overall survival of patients with both aggressive and indolent B-cell NHL that has been achieved following the addition of rituximab to conventional chemotherapy (4), not all patients who have CD20-positive tumors respond to the treatment (5, 6), and most patients who have disease response will relapse (7). More than 50% of patients with NHL will die of their disease (4–8). Since 2005, 5 new drugs have been approved for the treatment of lymphoma (6, 9), including 2 for B-cell NHL, namely, bortezomib, a proteasome inhibitor approved for the treatment of mantle cell lymphoma in 2006, and bendamustine, a DNA alkylating and antimetabolite agent approved for the treatment of indolent B-cell NHL in 2008. However, despite the large number of trials of novel agents, including monoclonal antibodies and small-molecule inhibitors (3, 10), there is still an important unmet medical need, particularly in second-line and subsequent lines of therapy. Concerning monoclonal antibodies, different modalities of conjugation have been tested in the clinic and have shown responses in hematological malignancies and NHL in particular, as discussed in this *CCR Focus* section, dedicated to antibody conjugates (11). These modalities include radionuclide conjugation (12), toxin conjugation (13), and small-molecule drug conjugation, also called antibody-drug conjugates (ADC; refs. 14–16). ADCs represent the most active field today, with at least 20 such ADCs in development (11). Very promising clinical responses have been achieved in both solid tumors, as shown by T-DM1 for the treatment of HER2-positive breast tumors (14), and hematological malignancies, as shown by SGN35 (15) and CMC-544 (16) for Hodgkin lymphoma and NHL, respectively.

Monoclonal Antibodies beyond Rituximab for Treating B-Cell Malignancies

Since the introduction of rituximab in 1997, only 2 more "naked" (nonconjugated) antibodies have been approved for the treatment of lymphoma: (i) alemtuzumab, an

Authors' Affiliations: [1]Oncology Business Division, Sanofi, Vitry sur Seine, France; [2]ImmunoGen, Inc., Waltham, Massachusetts

Corresponding Author: Véronique Blanc, Sanofi, 13 quai Jules Guesde, Vitry sur Seine, 94403 France. E-mail: Veronique.Blanc2@sanofi-aventis.com

doi: 10.1158/1078-0432.CCR-11-0485

©2011 American Association for Cancer Research.

Downloaded from clincancerres.aacrjournals.org on November 24, 2020. © 2011 American Association for Cancer Research.

anti-CD52 antibody approved in 2001 for the treatment of CLL (17); and (ii) ofatumumab, a second-generation anti-CD20 antibody displaying increased complement-dependent cytotoxicity compared with rituximab, that was approved in 2009 for relapse/refractory CLL patients who failed fludarabine and alemtuzumab (18). In addition to these 2 naked antibodies, 2 murine anti-CD20 radionuclide conjugates were approved for consolidation treatment in 2002 (^{90}Y-ibritumomab) and 2003 (^{131}I-tositumomab; refs. 12 and 19).

In recent years, investigators have made a considerable effort to further improve NHL treatment, and several second- and third-generation anti-CD20 monoclonal antibodies have been examined in clinical trials (20). In addition, exploration of other B-cell–specific antigens, including CD19, CD22, CD37, and CD40, as potential targets for the development of new antibody-based treatments is growing. Antibodies are being investigated as naked molecules, such as the anti-CD22 epratuzumab (21), the anti-CD40 dacetuzumab (22), and the different anti-CD19 antibodies (Table 1), or in an engineered format, such as the anti-CD19/anti-CD3–bispecific blinatumomab (23) and the anti-CD37–specific small modular immunopharmaceutical TRU-016 (24). The advent of ADC technologies has also led to clinical evaluation of conjugated antibodies, such as the anti-CD22-calicheamicin conjugate CMC544 (16) and the subject of this review, the anti-CD19-maytansinoid conjugate SAR3419 (25–28).

CD19 Antigen

CD19 is a type I transmembrane glycoprotein of the immunoglobulin Ig superfamily, with expression restricted to B cells (29). CD19 is involved in B-cell fate and differentiation through the modulation of B-cell receptor signaling at multiple stages of B-cell development (29, 30). CD19 is ubiquitously expressed on B cells (25), as it is found expressed from the early pre-B stage throughout B-cell differentiation up to mature B cells, before it is downmodulated at the plasma cell stage (Fig. 1). Thus, CD19 has broader expression than CD20. The pattern of CD19 expression is maintained in B-cell malignancies, covering all subtypes of B-cell lymphoma, from indolent to aggressive forms, as well as B-cell chronic lymphocytic leukemia and non-T acute lymphoblastic leukemia (31–33), and allows the targeting of tumor indications of early B cells, such as acute lymphoblastic leukemia (ALL), which cannot be targeted by rituximab. The quantification of the number of CD19 molecules at the surface of tumor cells and cell lines derived from malignant B cells resulted in a wide range of

Table 1. Clinical trials and discovery projects targeting CD19

Biologic compound	Type	Mechanism of action	Phase (initiation date)
MT-103 (blinatumomab) Micromet, Inc.	Bispecific scFv anti-CD19/anti-CD3 BiTE	T-cell recruitment and activation	I/II/III (2007) Pivotal trial for MDR$^+$ ALL
SAR3419 Sanofi-Aventis/ImmunoGen, Inc.	Humanized anti-CD19 mAb conjugated to maytansinoid DM4	ADC (tubulin binder)	I/II (2007)
MEDI-551 MedImmune/ Astra-Zeneca	Glycoengineered humanized anti-CD19 mAb (BioWa's Potelligent)	Naked antibody high-affinity FcγRIII-enhanced ADCC	I (2010)
MOR-208/XmAb5574 Xencor/Morphosys	Fc engineered humanized anti-CD19 mAb	Naked antibody high-affinity FcγRIII-enhanced ADCC	I (2010)
MDX-1342 Medarex/ Bristol-Myers Squibb	Glycoengineered fully human anti-CD19 mAb (BioWa's Potelligent)	Naked antibody high-affinity FcγRIII-enhanced ADCC	I (2008, on hold)
Combotox University of Texas Southwestern/Abiogen	Mixture of chimeric anti-CD19 mAb HD37 and anti-CD22 mAb RFB4, both conjugated to deglycosylated ricin A-chain (HD37-dgA + RFB4-dgA)	Immunotoxin conjugate with deglycosylated ricin A-chain	I (2005)
DI-B4 Merck KGaA/Cancer Research UK	Chimeric anti-CD19 mAb monoclonal antibody	Naked antibody ADCC	I (2010)
SGN-19A Seattle Genetics	Fully human anti-CD19 mAb (hBU12) conjugated to auristatin (vc-MMAE)	ADC (tubulin binder)	Discovery
MDX-1206 Medarex/ Bristol-Myers Squibb	Fully human anti-CD19 mAb (MDX1435) conjugated to duocarmycin (vc-MGBAA)	ADC (DNA alkylating agent)	Discovery
AFM-11 Affimed Therapeutics AG	Tetravalent tandem antibody (TandAb) anti-CD19/anti-CD3	T-cell recruitment	Discovery
AFM-12 Affimed Therapeutics AG	Tetravalent tandem antibody (TandAb) anti-CD19/anti-CD16	NK cell recruitment	Discovery

Downloaded from clincancerres.aacrjournals.org on November 24, 2020. © 2011 American Association for Cancer Research.

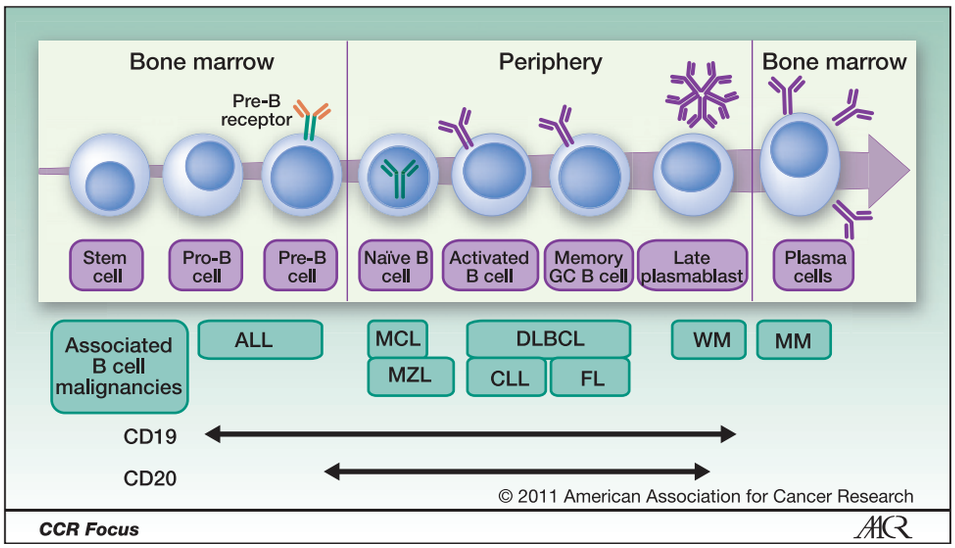

Figure 1. Pattern of expression of CD19 and CD20 antigens during B-cell development and associated malignancies. A simplified cartoon of B-cell lineage, B-cell malignancies, and antigen expression (59, 60). The positioning of the different B-cell malignancies associated with different stages of B-cell development is abridged and illustrative only; a detailed description is beyond the scope of this review.

published values due to differences in cell line clones, the antibodies studied, and the methodologies used. For example, CD19 expression was reported to be both >100,000 sites per cell (34) and ~10,000 sites per cell (35) for the same cellular models. In our hands, using a calibration curve of beads loaded with different amounts of human IgG1, the quantification of CD19 antigen at the surface of Ramos, Raji, and Daudi lymphoma cell lines gave average values of 42,166, 18,315, and 14,077 antibody-binding sites per cell, respectively. With the same assay, the quantification of CD19 on the surface of normal B lymphocytes yielded values in the range of 11,000 to 16,000 antibody-binding sites per cell, an order of magnitude similar to that of the lymphoma cell lines tested.

CD19 was shown to be internalized efficiently in lymphoma tumor models with the use of different antibodies, such as huB4 (35) and hBU12 (36). In our laboratories, we quantified the internalization and processing of the anti-CD19 antibody huB4 using an Alexa488 antibody conjugate and different tumor cell lines upon incubation at 37°C. The kinetics of appearance of antibody-free fluorescence, produced by lysosomal degradation of the antibody moiety, showed internalization and processing of the huB4-Alexa488 in all models, with some variability between models (35) that may reflect differences in the capacity of CD19 to internalize in different cellular contexts. Indeed, the level of CD21 coreceptor, expressed in a subset of lymphomas, was described to affect the internalization and efficacy of an anti-CD19-maytansinoid conjugate through a noncleavable linker (37). However, this observation was not confirmed in a second study using auristatin derivatives conjugated to a different anti-CD19 antibody through a cleavable linker (36).

Anti-CD19 Intervention

CD19's B-cell lineage–restricted expression and moderate to high homogeneous expression in most cases of lymphoma make it an attractive target for therapies for B-cell malignancies, as shown by the many previous and ongoing therapeutic interventions that focus on CD19 (Table 1). Different types of molecules targeting CD19 are being developed that can broadly fit into 3 main classes: (i) naked antibodies, most of which undergo modifications of their Fc portion to enhance binding to FcRγIII and subsequently enhance antibody-dependent cell-mediated cytotoxicity (ADCC) activity, such as MOR-208 and MEDI-551; (ii) bispecific antibodies with one arm binding to CD19 and one arm binding to either the T-cell receptor (as exemplified by blinatumomab, the most advanced anti-CD19 therapeutic molecule) or NK-cell receptors (as in the molecule AFM12, a tetravalent tandem antibody that is in the discovery stage of development); and (iii) antibody conjugates, for which anti-CD19 antibodies are conjugated to either a toxin (as exemplified by the ricin-based immunotoxin Combotox) or a potent low-molecular-weight cytotoxic molecule (as exemplified by SAR3419). As of today, Combotox has shown anticancer activity in NHL (38) and ALL (39) that may warrant further clinical testing. Studies of blinatumomab (23) and SAR3419 (27) have provided a clinical proof of concept, showing a notable rate of objective response in pretreated patients in phase I clinical trials.

SAR3419 Structure and Mechanism of Action

SAR3419 is an ADC that consists of a humanized monoclonal IgG1 antibody (huB4) attached to a highly potent tubulin inhibitor, the maytansinoid DM4 (40), through reaction with an optimized cleavable linker, *N*-succinimidyl-4-(2-pyridyldithio)butyrate (SPDB linker; Fig. 2). The succinimidyl group of the linker reacts with amino groups of lysine residues of the antibody to form stable amide bonds, and the pyridyldithio moiety reacts with the sulfhydryl group of DM4 to form a hindered disulfide bond between the linker and DM4. The disulfide bond can be cleaved inside target cells by thiol-disulfide

Downloaded from clincancerres.aacrjournals.org on November 24, 2020. © 2011 American Association for Cancer Research.

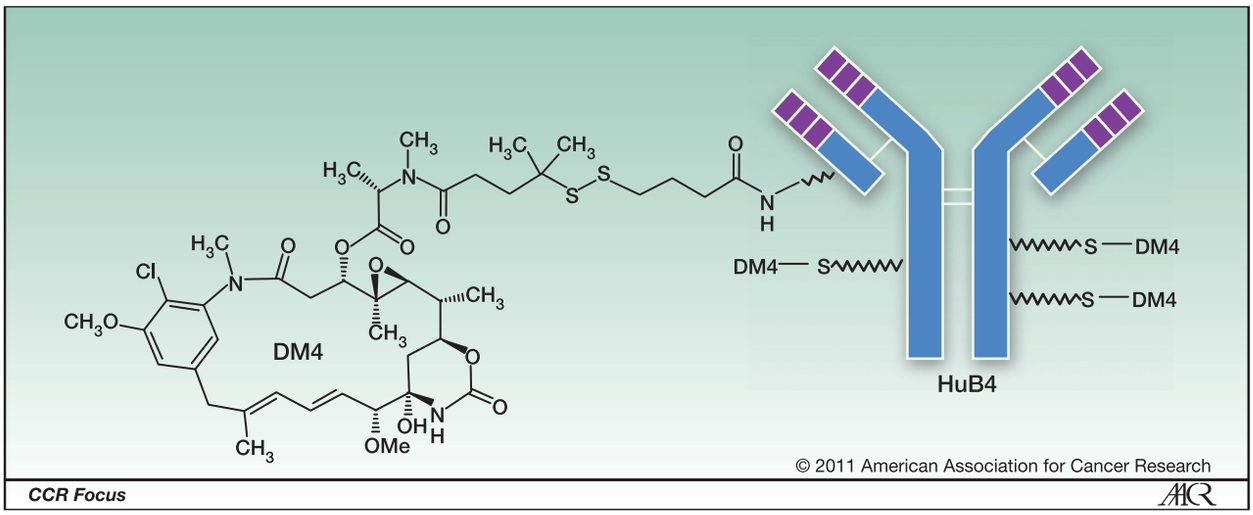

Figure 2. Structure of SAR3419. Figure is adapted from Al-Katib et al. (43).

exchange reactions to release fully active DM4 (28). SAR3419 contains an average of ~3.5 DM4 molecules per molecule of antibody.

The murine B4 antibody, one of the earliest antibodies to define the CD19 antigen (31), was humanized via a variable-domain resurfacing method (41) to yield huB4. The huB4 antibody displays a subnanomolar affinity for CD19 on the surface of B cells, and this affinity is conserved following conjugation to create SAR3419 (35). The huB4 antibody was shown to induce ADCC (data not shown) but not complement-dependent cytotoxicity as described for other anti-CD19 antibodies (42). The ADCC activity was conserved following conjugation to the maytansinoid. The naked antibody has no direct antiproliferative or proapoptotic activity. Therefore, huB4 was not found to be active *in vivo* as a single agent in severe combined immunodeficient (SCID) mice bearing several different lymphomas (43). The huB4 antibody binds only to the human CD19 antigen (29); it does not recognize CD19 in rodent or cynomolgus monkey toxicology models, and thus no B-cell depletion studies have been done with either the huB4 antibody or SAR3419 in animal models.

Maytansine and other maytansinoids are antimitotic agents that bind to tubulin, inhibiting microtubule assembly and inducing G_2/M arrest in the cell cycle, which subsequently leads to cell death (44). Maytansinoids are very potent, displaying cytotoxic activity in the 10 to 90 pmol/L range across several tumor cell lines, including lymphoma lines (45). The SPDB linker was selected based on its superior activity *in vivo* compared with SPP (another cleavable linker with a more labile disulfide bond) and the noncleavable SMCC linker in studies analogous to those described by Kellogg and colleagues (46) for another antibody-maytansinoid conjugate.

SAR3419 was shown to display potent *in vitro* cytotoxicity after 5 days of exposure to different CD19-positive lymphoma cell lines, with EC_{50} values ranging from subnanomolar to a few nanomolars (35). SAR3419 induced a rapid cell-cycle arrest at the G_2/M phase (within the first 24 hours of exposure) followed by an increase in apoptotic cells from 24 to 48 hours (35), as expected for delivery of the maytansinoid payload into CD19+ cells. As has been shown in the case of other maytansinoid conjugates (47) and in experiments with SAR3419 in which the DM4 moiety was radiolabeled (48), the mechanism of action of SAR3419 involves binding to the cell-surface antigen, followed by internalization via endocytosis and subsequent intracellular routing to lysosomes where the huB4 antibody moiety of the ADC is degraded to yield the lysine-SPDB-DM4 metabolite. Once it is in the reducing environment of the cytoplasm, this metabolite is further subjected to cleavage by thiol-disulfide exchange reactions to release the free maytansinoid thiol compound DM4 (47, 48). DM4 is then S-methylated to form *S*-methyl-DM4 by an endogenous S-methyl-transferase (47). The final metabolite of cancer cell metabolism of SAR3419, *S*-methyl-DM4, has a high potency as a microtubule poison that was shown to be similar to the potency of maytansine itself when compared in cytotoxicity assays *in vitro* on different tumor cell lines (40, 44, 49). The early metabolite formed upon lysosomal processing of the ADC, lysine-SPDB-DM4, shows a 1,000-fold lower activity on cell lines *in vitro* resulting from the negative effect of the charged lysine residue on its ability to diffuse across the plasma membrane into cells (47). However, such lysine-linker-maytansinoid species are potent microtubule poisons when they are released inside cells following uptake and lysosomal processing of an ADC (28, 47).

The mechanism of action of SAR3419 was also shown *in vivo* in immunodeficient SCID mice bearing human Ramos Burkitt's lymphoma, a model that was shown to be highly sensitive to SAR3419 (35). In recent studies done in our laboratories, SAR3419 was administered at a single dose of 20 mg/kg 14 days after tumor subcutaneous implantation. Tumor sampling was done at different times, and immunohistochemical evaluation of phospho-histone H3

Downloaded from clincancerres.aacrjournals.org on November 24, 2020. © 2011 American Association for Cancer Research.

(*p*-histone H3, a mitosis biomarker) and cleaved caspase 3 (a proapoptotic marker) was done. The single-dose treatment with SAR3419 induced a significant increase in staining for *p*-histone H3, revealing a mitosis blockade that was apparent 24 hours after administration (Fig. 3). This mitosis blockade was then followed by tumor cell apoptosis as evidenced 48 hours after dosing with the ADC by a marked increase in cells that stained positively for cleaved caspase 3 (Fig. 3).

Studies were also done in the same Ramos xenograft model to assess whether the pattern of metabolic processing observed in cell lines was the same as that seen in xenograft models. Mice bearing the tumor xenografts were injected with a single administration of radiolabeled [^{3}H]-SAR3419 (conjugate made with tritiated DM4) at 15 mg/kg in experiments similar to previous experiments involving another ADC with the same linker-maytansinoid design (49). Tumor sampling was done at different time points, and all metabolites were quantified. The total amount of low-molecular-weight (i.e., not protein-linked) metabolites increased rapidly from 2 to 8 hours, with a subsequent linear progression from 8 to 48 hours, and an overall 6-fold accumulation from 2 to 48 hours (Fig. 4). At the latter time point, 71% of the total radioactivity in the tumor xenograft corresponded to low-molecular-weight metabolites, in contrast to just 30% at 2 hours (data not shown). The processing of radiolabeled SAR3419 *in vivo* was found to be similar to the *in vitro* findings (Fig. 4), with the sequential formation of lysine-SPDB-DM4 (the major species at 2 hours) followed by DM4 (about 10% of total nonproteic metabolites at 2 hours, rising to ~24% at 8 hours) and then by the appearance of *S*-methyl-DM4 (first detected at 8 hours). As observed *in vitro*, similar quantities of lysine-SPDB-DM4 and *S*-methyl-DM4 were found in the tumors after 48 hours (Fig. 4; ref. 49). The time course of the formation of the active maytansinoid metabolites in the tumor is consistent with the observed high induction of *p*-histone H3 and cleaved caspase 3 at 24 and 48 hours, respectively (Fig. 3).

SAR3419 Preclinical Activities in Different Lymphoma Models

SAR3419 has shown *in vivo* efficacy in different lymphoma models, including Burkitt's lymphomas (Namalwa, Ramos, and Raji) and diffuse large B-cell lymphoma [DLBCL (RL, WSU-DLCL2, and WSU-FSCCL)] implanted in SCID mice (35, 43). In all models, SAR3419 showed a high level of activity leading to complete responses, with mice being tumor-free at study termination at the highest doses and with significant tumor growth delay at the lower doses (both when injected as a single dose and in a multiple-dose schedule).

As an illustration, in the Ramos lymphoma xenograft model (35), when treated by the intravenous route (2 doses with 4-day interval), SAR3419 was highly active at the dosage of 15 mg/kg (a well-tolerated dosage as evidenced by no loss in body weight), and 100% of the mice were tumor-free at the end of the study (day 124). The lower doses of 7.5 and 3.3 mg/kg were also highly active, with complete tumor regressions in 100% of the animals and with 5 out of 7 mice being tumor-free at the dose of 7.5 mg/kg on day 124. In comparison, treatment with unconjugated DM4 at a dose equivalent to the 15 mg/kg dose of SAR3419 (0.35 mg/kg of DM4, 2 doses with 4-day interval) showed no significant antitumor activity, indicating that conjugation of the DM4 to the antibody was critical for delivering sufficient maytansinoid to the cancer cells *in vivo* to induce tumor shrinkage.

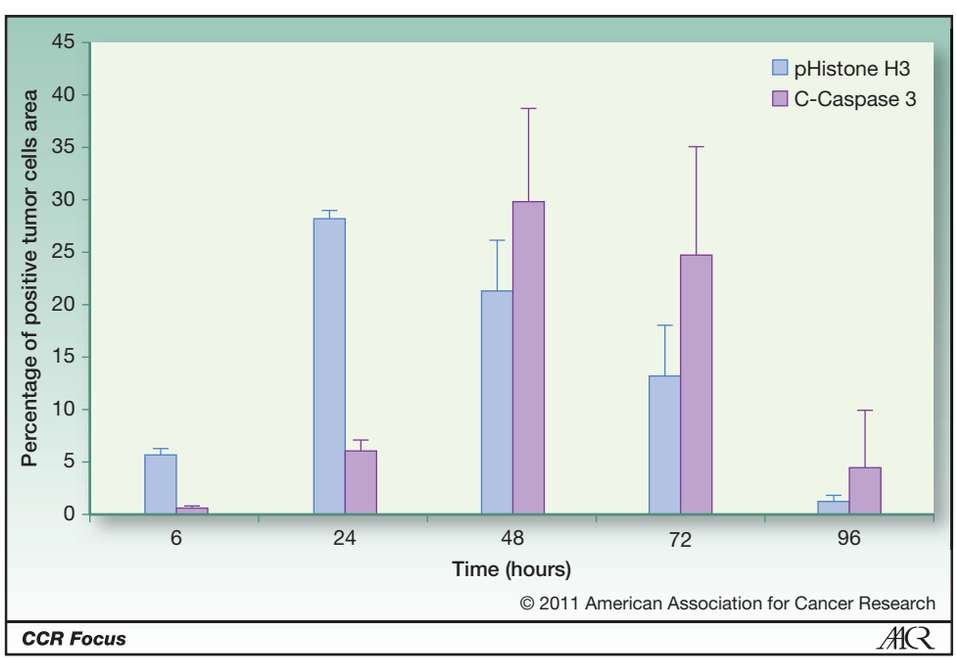

Figure 3. Kinetics of pharmacodynamic markers *p*-histone H3 and cleaved caspase 3 (C-Caspase 3) in Ramos xenograft model. Quantitative evaluation of *p*-Histone H3 and C-Caspase 3 by image analysis quantification at 6, 24, 48, 72, and 96 hours after administration of a single intravenous dose of 20 mg/kg of SAR3419 in SCID mice bearing established Ramos subcutaneous xenograft tumors.

Downloaded from clincancerres.aacrjournals.org on November 24, 2020. © 2011 American Association for Cancer Research.

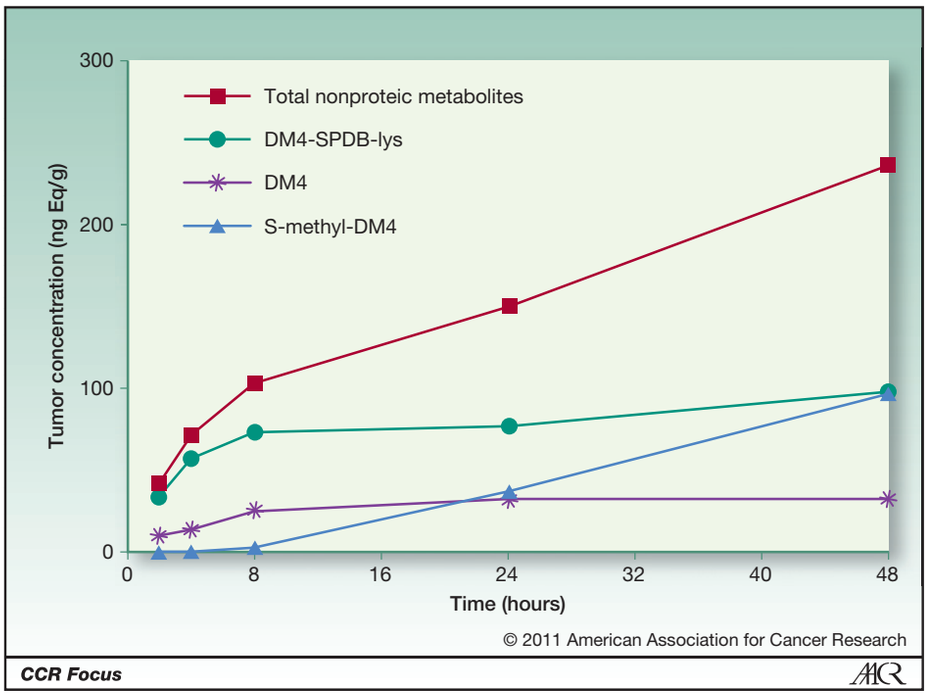

Figure 4. Kinetics of the production of nonproteic maytansinoid metabolites in the Ramos xenograft model. Quantitative evaluation of nonproteic maytansinoid metabolites (metabolites not linked to proteins) in nanograms per gram of tumor (ng Eq/g) at 2, 6, 8, 24, and 48 hours after administration of a single intravenous dose of 15 mg/kg of [^{3}H]-SAR3419 in SCID mice bearing established Ramos xenograft tumors.

The specificity of tumor targeting by SAR3419 was further shown by comparing the efficacy of a 10 mg/kg single dose of SAR3419 with the efficacy of the same dose of SAR3419 administered together with 50 mg/kg of naked huB4 antibody. The coadministration of SAR3419 with excess huB4 antibody resulted in complete abrogation of the antitumor activity of SAR3419, because binding of the naked huB4 antibody to the CD19 antigen blocks binding of the conjugate to its target (Fig. 5). Coadministration of SAR3419 with an excess of a nonspecific humanized IgG1 control antibody (huMy9-6) had no effect on blocking the antitumor activity of SAR3419 (Fig. 5).

SAR3419 was tested in a systemic model of DLBCL in which animals that were injected intravenously with the WSU-FSCCL cell line developed disseminated disease with bone marrow, liver, spleen, lymph node, and central nervous system involvement (43). In this model, SAR3419 also showed a dose-response relationship (2 doses with 4-day interval), with all animals surviving at the end of the experiment (150 days postdose) at 30 mg/kg, the highest dose tested. In the control group, all mice were euthanized between day 60 and day 73 because they showed a large burden of disseminated tumor. At the lower dose groups of 15 mg/kg and 7.5 mg/kg, 4 out of 7 mice and 2 out of 7 mice, respectively, survived until day 150 (43). In contrast, there was no activity of the naked huB4 injected at 30 mg/kg (2 doses with 4-day interval) or 0.6 mg/kg of DM4 (2 doses with 4-day interval), corresponding to the amount of DM4 in the highest SAR3419 dose of 30 mg/kg.

Taken together, the preclinical results show a high and specific activity of SAR3419 in a variety of different lymphoma models. The results highlight the role of conjugation in directing the cytotoxic molecule to the tumor, allowing delivery of enough DM4 *in vivo* to induce tumor regression. It confers a large therapeutic window to a cytotoxic molecule that otherwise would be too toxic to be used alone (50), with free maytansine having little or no activity in most tumor models at its maximum tolerated dose (MTD; refs. 35, 43, and 45). In addition, the activity of SAR3419 compared favorably with rituximab or CHOP treatments in the DLBCL model tested, suggesting opportunities for future improvements in lymphoma treatment (43).

Imaging SAR3419 Activity in a Mouse Model

Metabolic imaging with fluorodeoxyglucose positron emission tomography (FDG-PET) combined with computed tomography is widely accepted for staging of lymphoma patients and assessment of response after completion of therapy. It is now being used to monitor response during treatment in lymphoma patients (51). We therefore investigated whether FDG uptake in tumor is an appropriate noninvasive readout for monitoring response and predicting outcome of SAR3419 therapy in a disseminated model of lymphoma. Mice inoculated with human Daudi lymphoma cells were followed longitudinally by FDG-PET. At an advanced stage of disease, involvement of kidney, ovary, and spinal cord sites was evident in all mice 23 days after cell inoculation (Fig. 6), and the PET signal was used to randomize the mice at baseline before treatment with 12.5 mg/kg SAR3419. In comparison with the control group, the metabolic activity in tumor-invaded regions was reduced by 50% after treatment (Fig. 6). The response to SAR3419 seemed to be homogeneous, with a decrease of signal in

Downloaded from clincancerres.aacrjournals.org on November 24, 2020. © 2011 American Association for Cancer Research.

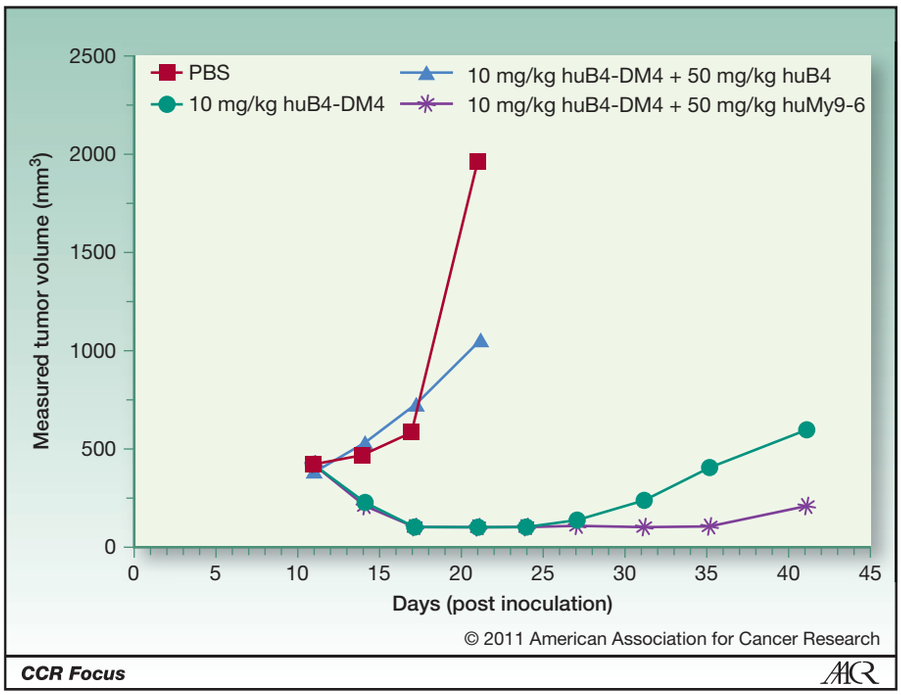

Figure 5. Impact of naked huB4 antibody on the efficacy of a single administration of SAR3419 against a bulky Ramos subcutaneous tumor xenograft model. SCID mice were inoculated with Ramos tumor cells, and once the xenografts had reached about 295 mm^3 on day 11, mice (6 per group) were treated with a test article given by intravenous injection (tail vein). The huMy9-6 (anti-CD33 antibody) is an isotype-matched, nonspecific control humanized IgG1 antibody; huB4 is the anti-CD19 humanized IgG1 antibody moiety of SAR3419; huB4-DM4 is a synonym for SAR3419.

all invaded sites, including the spinal cord. This decrease in PET signal translated into prolonged survival for the mice in the treated group, with a 40% median increase in lifespan. In a separate experiment, modulation of the metabolic signal was used to adapt the treatment schedule. The mice were injected twice with 15 mg/kg SAR3419 with a 5-day interval between both injections. Within 5 days after the start of therapy, the metabolic activity had decreased to background values. The PET signal then recurred and increased to reach the initial values 15 days after the end of the first cycle, showing relapse of the disease. A second cycle of treatment was then administered and was shown to control the disease, as evidenced by the stabilization of the PET signal for 15 additional days. Again, the modulation of the PET signal by SAR3419 therapy was predictive of outcome, with a ~175% increase in lifespan for treated mice. Serial imaging of tumor uptake of FDG can therefore serve as a translational efficacy readout for SAR3419 therapy.

SAR3419 Clinical Development

Two phase I dose escalation studies exploring 2 different schedules of administration [every 3 weeks (Q3W; ref. 27) and weekly (Q1W; ref. 52)] have been conducted with SAR3419 in patients with refractory/relapsed B-cell NHL expressing CD19.

The preliminary results from the Q3W trial, in which patients were eligible for up to 6 cycles of treatment, showed that the MTD was 160 mg/m^2 (~4.3 mg/kg), a dose level that was subsequently used to treat an expanded cohort of 20 patients (27). The dose-limiting toxicity (DLT) at doses > 200 mg/m^2 was reversible toxicity to the cornea that did not preclude continued dosing (at 208 mg/m^2) in patients receiving clinical benefit, albeit with dose delays of 1 to 2 weeks (27). This ocular toxicity, which consisted mainly of blurred vision, was associated with microcystic epithelial corneal changes and was typically seen after cycle 2 or later cycles. The DLT observed in this Q3W phase I study of SAR3419 is similar to that observed in phase I studies of albumin-bound paclitaxel (53), as well as one other ADC compound from among the several ADCs in clinical evaluation that have the same SPDB-DM4 linker-maytansinoid format (28, 54). No other clinically significant grade 3 or 4 toxicities exceed an incidence of 10%, including peripheral neuropathy and gastrointestinal toxicities that are classically seen with agents targeting tubulin (27). As with other antibody-maytansinoid conjugates (28), there were no clinically significant hematologic toxicities, and no gastrointestinal toxicities were reported at the MTD, showing the efficacy of the linker between the huB4 antibody and the DM4 in the blood stream [the toxicities of free maytansine included myelosuppression and severe gastrointestinal toxicities (50)]. The half-life of SAR3419 in these patients was 4 to 6 days and was approximately linear across all doses from 20 mg/m^2 to 270 mg/m^2 in the phase I trial (27). This suggests that there was a negligible antigen sink from normal tissue expression, as might be anticipated for a population of heavily pretreated patients with NHL, all of whom had received prior therapy with rituximab, which effectively depletes normal B cells.

Tumor shrinkage was observed in more than half of the 35 response-evaluable patients (74%) at the time of initial reporting of the study, with 6 objective responses (27). Of note, 7 of 15 patients with rituximab-refractory disease showed tumor shrinkage, with 1 objective response. Although these are early results from a phase I trial that

Downloaded from clincancerres.aacrjournals.org on November 24, 2020. © 2011 American Association for Cancer Research.

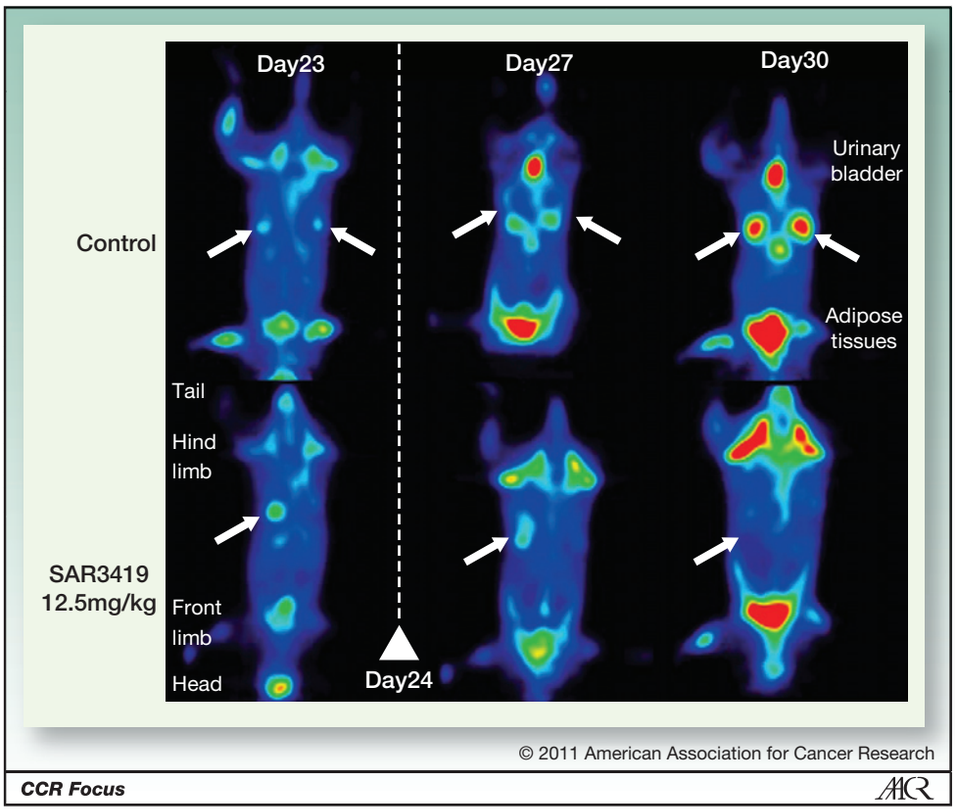

Figure 6. Longitudinal monitoring of SAR3419 activity using FDG-PET in mice inoculated intravenously with Daudi lymphoma. Samples of serial FDG-PET images obtained in mice bearing disseminated lymphoma treated on day 24 with SAR3419 or control treatment. The metabolic activity is coded on a color scale from blue (low radioactive tracer uptake) to red (high uptake). The tracer accumulates in elimination organs (urinary bladder), nonspecific sites (adipose tissues), and FDG-avid tumor tissues (depicted by white arrows).

need to be confirmed and extended by further studies, they nevertheless show promising activity and tolerability, especially considering the wide dose range (10–270 mg/m^2), the pretreated patient population, and the mixed histology of the enrolled patients (27). Tumor shrinkage was seen in a variety of lymphoma subtypes, including DLBCL, with objective responses noted in follicular lymphoma and marginal zone lymphoma at the time of initial reporting of the study (27). One might expect normal B cells to be depleted by SAR3419 just as both normal and malignant B cells are depleted upon treatment with anti-CD20 antibodies. Indeed, both normal B cells and cells of B-cell malignancies have similar levels of cell-surface expression of the CD19 antigen, as discussed above. However, in the patients treated in the phase I studies, the basal lymphocyte count was usually extremely low because of the many prior lines of therapy given, including prior treatment with rituximab, which results in prolonged B-cell depletion. Thus, given the patients' preexisting B-cell depletion at the time of study entry, we can draw no conclusions regarding normal B-cell depletion upon treatment with SAR3419 from the 2 phase I clinical studies reported to date.

A second study with a weekly dosing schedule was undertaken that established an MTD of 55 mg/m^2 (52). The dose intensity reached was similar to that obtained with the Q3W schedule. An expanded cohort of 16 patients was evaluated at this dose level. Patients were eligible for up to 8 weekly cycles of treatment in this study, with the possibility of a further 4 cycles if warranted for clinical benefit. Although ocular toxicity was noted on this dosing regimen, with a late onset (mainly postcycle 7 or 8), the incidence and severity of the observations was markedly reduced relative to the Q3W schedule, with only 2% grade 3 or 4 on the Q1W schedule. A modified schedule, based on pharmacokinetic simulations, consisting of 4 weekly doses of 55 mg/m^2 followed by 4 biweekly doses, is currently being explored in an attempt to further decrease the incidence of this toxicity. This type of schedule was successfully achieved in the phase III trial of albumin-bound paclitaxel, because it abrogated the reversible toxicity to the cornea that defined the DLT in phase I (55).

As in the Q3W study, the incidence and severity of hematologic toxicity was clinically insignificant at the 55 mg/m^2 dose. Not only is the Q1W schedule well tolerated, it also seems to offer superior activity relative to the Q3W schedule, with the majority of patients showing a reduction in their lymphoma during treatment with SAR3419, and with a 33% objective response rate. Again, this is a highly encouraging signal of activity in a heavily pretreated phase I population of patients with mixed histology and treated

Downloaded from clincancerres.aacrjournals.org on November 24, 2020. © 2011 American Association for Cancer Research.

across a wide dose range from 10 mg/m^2 to 70 mg/m^2 (52). Overall, these encouraging preliminary data indicate that SAR3419 offers a very promising new modality for treating B-cell malignancies and show that targeting CD19 with an ADC is a viable therapeutic option that is worth further exploration.

Conclusions

For over 10 years, rituximab has been positively influencing lymphoma treatment. It has good potency and an excellent toxicity profile, thanks to the B-cell–restricted expression of CD20. However, a significant number of patients relapse, and in the effort to improve therapy, investigators are exploring multiple strategies in clinical and discovery research for targeting B-cell lymphomas using monoclonal antibodies directed to B-cell antigens. In addition to CD20, several other B-cell–specific antigens are suitable for targeted therapy, including CD19 and CD22 (13, 16, 21, 26, 36, 43). CD19 is the target that was exploited in developing SAR3419, an ADC designed to deliver a potent tubulin poison, the maytansinoid DM4, to malignant B cells. The highly restricted expression of CD19 for B cells has the potential to allow effective treatment of B-cell malignancies with SAR3419, without toxicity to other hematologic non–B-cell compartments. An ADC directed to a less restricted target that is also expressed on immune cells other than B cells (e.g., CD52, the target for alemtuzumab) would be more likely to exhibit broad hematologic toxicity.

Clinical proof-of-concept for ADCs armed with tubulin inhibitor payloads was recently shown in both HER2+ metastatic breast cancer by T-DM1 (14, 56), a maytansinoid conjugate of trastuzumab targeting HER2, and in lymphoma by SGN35 (15, 57), an anti-CD30 monoclonal antibody conjugated to an auristatin derivate. SGN35 has shown high response rates in both Hodgkin lymphoma and anaplastic large-cell lymphoma (15, 57), raising hope for pursuing such approaches in hematological malignancies. In the case of SGN35, it is clear that conjugation of the antibody to a tubulin-inhibitor cytotoxic molecule has produced an ADC molecule with a very good response rate in clinical studies for a target that has shown no such activity with the unconjugated naked anti-CD30 antibody (58). In the case of anti-CD19 antibodies, it is too early to tell whether any of the naked antibodies in development (see Table 1) will achieve a good response rate in the clinic. Studies of the bifunctional anti-CD19/anti-CD3 molecule blinatumomab have shown proof-of-concept of T-cell activation using CD19 targeting in ALL and NHL, but the treatment regimen still requires optimization to reduce the frequency of adverse events, particularly in NHL (23).

The preliminary clinical activity shown by SAR3419 in 2 phase I clinical trials is encouraging for its future development (27, 52). Objective responses were seen in both follicular lymphoma and DLBCL. No clinically significant hematological toxicity was observed, and the ocular toxicity that defined the DLT on the Q3W schedule seemed to be manageable on an alternative dosing regimen.

Nevertheless, although the phase I data are promising, there are still several challenges to overcome before we can fully assess the potential of this new molecule. What would be the efficacy if it were used in earlier lines of treatment? In the case of T-DM1 in metastatic breast cancer (14), early clinical data suggest that the response rate in a first-line setting improves upon that seen in heavily pretreated patients. However, in the case of NHL, strategies to assess new agents in early lines of treatment can be challenging given the relatively good outcomes of first-line treatment regimens. Another development challenge is to assess the significance of drug resistance. What is the propensity for NHL to become resistant to the killing mechanism of a tubulin agent (especially after prior CHOP, which includes a vinca alkaloid), and how does it affect the response rate obtained so far? During clinical development, it will also be important to assess the relationship of the response rate to the level of antigen expression: Although CD19 expression is a marker for B cells, its expression level may vary from one B-cell lymphoma to another. Will we need to stratify patients with respect to antigen expression level? Another question to address during development is how the cell-cycle status of the lymphoma influences the response to SAR3419, given that tubulin agents are mainly active on dividing cells. These questions and challenges will be further addressed during phase II trials, allowing us to understand the full potential of SAR3419. The phase II program to develop SAR3419 in B-cell malignancies will start in the second half of 2011 and will include a robust assessment of activity in patients with relapsed DLBCL, a patient population that showed responses in phase I trials and that has a clear, unmet medical need.

Disclosure of Potential Conflicts of Interest

No potential conflicts of interest were disclosed.

Acknowledgments

The authors thank Patrick Soubayrol, Toni Cordeiro, Souad Naimi, Patricia Vrignaud, Marie-Laure Ozoux, Ingrid Sassoon, Marie-Cécile Wetzel, Laurent Besret, and Christoph Lengauer for their contributions to the work presented here.

Received May 24, 2011; revised July 18, 2011; accepted August 15, 2011; published online October 14, 2011.

References

1. American Cancer Society [homepage on the Internet]. Cancer Facts and Figures 2010. Atlanta, GA: American Cancer Society 2010 [cited 2011 Sept 13]. Available from: http://www.cancer.org/acs/groups/content/@nho/documents/document/acspc-024113.pdf.

Downloaded from clincancerres.aacrjournals.org on November 24, 2020. © 2011 American Association for Cancer Research.

2. Nogai H, Dörken B, Lenz G. Pathogenesis of non-Hodgkin's lymphoma. J Clin Oncol 2011;29:1803–11.
3. Maloney D, Morschhauser F, Linden O, Hagenbeek A, Gisselbrecht C. Diversity in antibody-based approaches to non-Hodgkin lymphoma. Leuk Lymphoma 2010;51[Suppl 1]:20–7.
4. Pulte D, Gondos A, Brenner H. Ongoing improvement in outcomes for patients diagnosed as having non-Hodgkin lymphoma from the 1990s to the early 21st century. Arch Intern Med 2008;168: 469–76.
5. McLaughlin P, Grillo-López AJ, Link BK, Levy R, Czuczman MS, Williams ME, et al. Rituximab chimeric anti-CD20 monoclonal antibody therapy for relapsed indolent lymphoma: half of patients respond to a four-dose treatment program. J Clin Oncol 1998;16:2825–33.
6. Zelenetz AD, Abramson JS, Advani RH, Andreadis CB, Byrd JC, Czuczman MS, et al. NCCN Clinical Practice Guidelines in Oncology: non-Hodgkin's lymphomas. J Natl Compr Canc Netw 2010;8: 288–334.
7. Davis TA, Grillo-López AJ, White CA, McLaughlin P, Czuczman MS, Link BK, et al. Rituximab anti-CD20 monoclonal antibody therapy in non-Hodgkin's lymphoma: safety and efficacy of re-treatment. J Clin Oncol 2000;18:3135–43.
8. Friedberg JW, Fisher RI. Diffuse large B-cell lymphoma. Hematol Oncol Clin North Am 2008;22:941–52, ix.
9. Younes A. Beyond chemotherapy: new agents for targeted treatment of lymphoma. Nat Rev Clin Oncol 2011;8:85–96.
10. Mahadevan D, Fisher RI. Novel therapeutics for aggressive non-Hodgkin's lymphoma. J Clin Oncol 2011;29:1876–84.
11. Teicher BA, Chari RVJ. Antibody conjugate therapeutics: challenges and potential. Clin Cancer Res 2011;17:6389–97.
12. Steiner M, Neri D. Antibody-radionuclide conjugates for cancer therapy: historical considerations and new trends. Clin Cancer Res 2011;17:6406–16.
13. Kreitman RJ, Pastan I. Antibody fusion proteins: anti-CD22 recombinant immunotoxin moxetumomab pasudotox. Clin Cancer Res 2011;17:6398–405.
14. LoRusso PM, Weiss D, Guardino E, Girish S, Sliwkowski MX. Trastuzumab emtansine: a unique antibody-drug conjugate in development for human epidermal growth factor receptor 2–positive cancer. Clin Cancer Res 2011;17:6437–47.
15. Katz J, Janik JE, Younes A. Brentuximab vedotin (SGN-35). Clin Cancer Res 2011;17:6428–36.
16. Ricart AD. Antibody-drug conjugates of calicheamicin derivative: gemtuzumab ozogamicin and inotuzumab ozogamicin. Clin Cancer Res 2011;17:6417–27.
17. Fraser G, Smith CA, Imrie K, Meyer R, et al. Alemtuzumab in chronic lymphocytic leukemia. Curr Oncol 2007;14:96–109.
18. Nabhan C, Kay NE. The emerging role of ofatumumab in the treatment of chronic lymphocytic leukemia. Clin Med Insights Oncol 2011;5: 45–53.
19. Beck A, Wurch T, Bailly C, Corvaia N. Strategies and challenges for the next generation of therapeutic antibodies. Nat Rev Immunol 2010;10:345–52.
20. Czuczman MS, Gregory SA. The future of CD20 monoclonal antibody therapy in B-cell malignancies. Leuk Lymphoma 2010;51:983–94.
21. Leonard JP, Goldenberg DM. Preclinical and clinical evaluation of epratuzumab (anti-CD22 IgG) in B-cell malignancies. Oncogene 2007;26:3704–13.
22. Furman RR, Forero-Torres A, Shustov A, Drachman JG. A phase I study of dacetuzumab (SGN-40, a humanized anti-CD40 monoclonal antibody) in patients with chronic lymphocytic leukemia. Leuk Lymphoma 2010;51:228–35.
23. Nagorsen D, Baeuerle PA. Immunomodulatory therapy of cancer with T cell-engaging BiTE antibody blinatumomab. Exp Cell Res 2011;317: 1255–60.
24. Zhao X, Lapalombella R, Joshi T, Cheney C, Gowda A, Hayden-Ledbetter MS, et al. Targeting CD37-positive lymphoid malignancies with a novel engineered small modular immunopharmaceutical. Blood 2007;110:2569–77.
25. Advani A, Coiffier B, Czuczman MS, Dreyling M, Foran J, Gine E, et al. Safety, pharmacokinetics, and preliminary clinical activity of inotuzumab ozogamicin, a novel immunoconjugate for the treatment of B-cell non-Hodgkin's lymphoma: results of a phase I study. J Clin Oncol 2010;28:2085–93.
26. Polson AG, Ho WY, Ramakrishnan V. Investigational antibody-drug conjugates for hematological malignancies. Expert Opin Investig Drugs 2011;20:75–85.
27. Younes A, Gordon L, Kim S, Romaguera J, Copeland AR, de Castro Farial S, et al. Phase I multi-dose escalation study of the anti-CD19 maytansinoid immunoconjugate SAR3419 administered by intravenous (IV) infusion every 3 weeks to patients with relapsed/refractory B-cell non-Hodgkin's lymphoma (NHL). Blood (ASH Annual Meeting Abstracts) 2009;114:585.
28. Lambert JM. Antibody-maytansinoid conjugates: a new strategy for the treatment of cancer. Drugs Future 2010;35:471–80.
29. Del Nagro CJ, Otero DC, Anzelon AN, Omori SA, Kolla RV, Rickert RC. CD19 function in central and peripheral B-cell development. Immunol Res 2005;31:119–31.
30. de Rie MA, Schumacher TN, van Schijndel GM, van Lier RA, Miedema F. Regulatory role of CD19 molecules in B-cell activation and differentiation. Cell Immunol 1989;118:368–81.
31. Nadler LM, Anderson KC, Marti G, Bates M, Park E, Daley JF, et al. B4, a human B lymphocyte-associated antigen expressed on normal, mitogen-activated, and malignant B lymphocytes. J Immunol 1983;131:244–50.
32. Scheuermann RH, Racila E. CD19 antigen in leukemia and lymphoma diagnosis and immunotherapy. Leuk Lymphoma 1995;18:385–97.
33. Anderson KC, Bates MP, Slaughenhoupt BL, Pinkus GS, Schlossman SF, Nadler LM. Expression of human B cell-associated antigens on leukemias and lymphomas: a model of human B cell differentiation. Blood 1984;63:1424–33.
34. Du X, Beers R, Fitzgerald DJ, Pastan I. Differential cellular internalization of anti-CD19 and -CD22 immunotoxins results in different cytotoxic activity. Cancer Res 2008;68:6300–5.
35. Lutz RJ, Zuany-Amorim C, Vrignaud P, Mayo MF, Guerif S, Xie H, et al. Preclinical evaluation of SAR3419 (huB4-DM4), an anti-CD19-maytansinoid immunoconjugate, for the treatment of B-cell lymphoma. Proc Am Assoc Cancer Res 2006;47:3731.
36. Gerber HP, Kung-Sutherland M, Stone I, Morris-Tilden C, Miyamoto J, McCormick R, et al. Potent antitumor activity of the anti-CD19 auristatin antibody drug conjugate hBU12-vcMMAE against rituximab-sensitive and -resistant lymphomas. Blood 2009;113:4352–61.
37. Ingle GS, Chan P, Elliott JM, Chang WS, Koeppen H, Stephan J-P, et al. High CD21 expression inhibits internalization of anti-CD19 antibodies and cytotoxicity of an anti-CD19-drug conjugate. Br J Haematol 2008;140:46–58.
38. Messmann RA, Vitetta ES, Headlee D, Senderowicz AM, Figg WD, Schindler J, et al. A phase I study of combination therapy with immunotoxins IgG-HD37-deglycosylated ricin A chain (dgA) and IgG-RFB4-dgA (Combotox) in patients with refractory CD19(+), CD22(+) B cell lymphoma. Clin Cancer Res 2000;6:1302–13.
39. Herrera L, Bostrom B, Gore L, Sandler E, Lew G, Schlegel PG, et al. A phase 1 study of Combotox in pediatric patients with refractory B-lineage acute lymphoblastic leukemia. J Pediatr Hematol Oncol 2009;31:936–41.
40. Widdison WC, Wilhelm SD, Cavanagh EE, Whiteman KR, Leece BA, Kovtun Y, et al. Semisynthetic maytansine analogues for the targeted treatment of cancer. J Med Chem 2006;49:4392–408.
41. Roguska MA, Pedersen JT, Keddy CA, Henry AH, Searle SJ, Lambert JM, et al. Humanization of murine monoclonal antibodies through variable domain resurfacing. Proc Natl Acad Sci U S A 1994;91: 969–73.
42. Jaglowski SM, Alinari L, Lapalombella R, Muthusamy N, Byrd JC. The clinical application of monoclonal antibodies in chronic lymphocytic leukemia. Blood 2010;116:3705–14.
43. Al-Katib AM, Aboukameel A, Mohammad R, Bissery M-C, Zuany-Amorim C. Superior antitumor activity of SAR3419 to rituximab in xenograft models for non-Hodgkin's lymphoma. Clin Cancer Res 2009;15:4038–45.
44. Lopus M, Oroudjev E, Wilson L, Wilhelm S, Widdison W, Chari R, et al. Maytansine and cellular metabolites of antibody-maytansinoid

Downloaded from clincancerres.aacrjournals.org on November 24, 2020. © 2011 American Association for Cancer Research.

conjugates strongly suppress microtubule dynamics by binding to microtubules. Mol Cancer Ther 2010;9:2689–99.
45. Chari RV, Martell BA, Gross JL, Cook SB, Shah SA, Blättler WA, et al. Immunoconjugates containing novel maytansinoids: promising anticancer drugs. Cancer Res 1992;52:127–31.
46. Kellogg BA, Garrett L, Kovtun Y, Lai KC, Leece B, Miller M, et al. Disulfide-linked antibody-maytansinoid conjugates: optimization of *in vivo* activity by varying the steric hindrance at carbon atoms adjacent to the disulfide linkage. Bioconjug Chem 2011;22:717–27.
47. Erickson HK, Park PU, Widdison WC, Kovtun YV, Garrett LM, Hoffman K, et al. Antibody-maytansinoid conjugates are activated in targeted cancer cells by lysosomal degradation and linker-dependent intracellular processing. Cancer Res 2006;66:4426–33.
48. Erickson HK, Provenzano CA, Mayo MF, Widdison WC, Audette C, Leece B, et al. Target-cell processing of the anti-CD19 antibody maytansinoid conjugate SAR3419 in preclinical models [abstract]. In: Proceedings of the 100th Annual Meeting of the American Association for Cancer Research; 2009 Apr 18–22; Denver, CO. Philadelphia (PA): AACR; 2009. Abstract nr 5473.
49. Erickson HK, Widdison WC, Mayo MF, Whiteman K, Audette C, Wilhelm SD, et al. Tumor delivery and *in vivo* processing of disulfide-linked and thioether-linked antibody-maytansinoid conjugates. Bioconjug Chem 2010;21:84–92.
50. Issell BF, Crooke ST. Maytansine. Cancer Treat Rev 1978;5:199–207.
51. Juweid ME. FDG-PET/CT in lymphoma. Methods Mol Biol 2011;727:1–19.
52. Coiffier B, Ribrag V, Dupuis J, Tilly H, Haioun C, Morschhauseret F, et al. Phase I/II study of the anti-CD19 maytansinoid immunoconjugate SAR3419 administered weekly to patients with relapsed/refractory B-cell non-Hodgkin's lymphoma (NHL). J Clin Oncol 2011;29 (suppl):8017.
53. Ibrahim NK, Desai N, Legha S, Soon-Shiong P, Theriault RL, Rivera E, et al. Phase I and pharmacokinetic study of ABI-007, a Cremophor-free, protein-stabilized, nanoparticle formulation of paclitaxel. Clin Cancer Res 2002;8:1038–44.
54. Qin A, Watermill J, Mastico RA, Lutz RJ, O'Keeffe J, Zildjian S, et al. The pharmacokinetics and pharmacodynamics of IMGN242 (huC242-DM4) in patients with CanAg-expressing solid tumors. J Clin Oncol 2008;26(15S):3066.
55. Gradishar WJ, Tjulandin S, Davidson N, Shaw H, Desai N, Bhar P, et al. Phase III trial of nanoparticle albumin-bound paclitaxel compared with polyethylated castor oil-based paclitaxel in women with breast cancer. J Clin Oncol 2005;23:7794–803.
56. Burris HA 3rd, Rugo HS, Vukelja SJ, Vogel CL, Borson RA, Limentani S, et al. Phase II study of the antibody drug conjugate trastuzumab-DM1 for the treatment of human epidermal growth factor receptor 2 (HER2)-positive breast cancer after prior HER2-directed therapy. J Clin Oncol 2011;29:398–405.
57. Younes A, Bartlett NL, Leonard JP, Kennedy DA, Lynch CM, Sievers EL, et al. Brentuximab vedotin (SGN35) for relapsed CD30-positive lymphomas. N Engl J Med 2011;363:1812–21.
58. Foyil KV, Bartlett NL. Anti-CD30 antibodies for Hodgkin lymphoma. Curr Hematol Malig Rep 2010;5:140–7.
59. Janeway C, Travers P, Walport M, Shlomchik MJ. Immunobiology: the immune system in health and disease. 6th ed. New York: Garland Publishing; 2004.
60. Uckun FM. Regulation of human B-cell ontogeny. Blood 1990;76: 1908–23.

Downloaded from clincancerres.aacrjournals.org on November 24, 2020. © 2011 American Association for Cancer Research.

AACR American Association for Cancer Research

Clinical Cancer Research

SAR3419: An Anti-CD19-Maytansinoid Immunoconjugate for the Treatment of B-Cell Malignancies

Veronique Blanc, Anne Bousseau, Anne Caron, et al.

Clin Cancer Res 2011;17:6448-6458.

Updated version Access the most recent version of this article at:
http://clincancerres.aacrjournals.org/content/17/20/6448

Cited articles This article cites 57 articles, 28 of which you can access for free at:
http://clincancerres.aacrjournals.org/content/17/20/6448.full#ref-list-1

Citing articles This article has been cited by 22 HighWire-hosted articles. Access the articles at:
http://clincancerres.aacrjournals.org/content/17/20/6448.full#related-urls

E-mail alerts Sign up to receive free email-alerts related to this article or journal.

Reprints and Subscriptions To order reprints of this article or to subscribe to the journal, contact the AACR Publications Department at pubs@aacr.org.

Permissions To request permission to re-use all or part of this article, use this link
http://clincancerres.aacrjournals.org/content/17/20/6448.
Click on "Request Permissions" which will take you to the Copyright Clearance Center's (CCC) Rightslink site.

Downloaded from clincancerres.aacrjournals.org on November 24, 2020. © 2011 American Association for Cancer Research.